F.I.A.T. FINAL REPORT No. 610

DIMENSIONING OF DIRECTIONAL ANTENNAS.

Report prepared by

FIELD INFORMATION AGENCY, TECHNICAL
UNITED STATES GROUP CONTROL COUNCIL FOR GERMANY

BRITISH INTELLIGENCE OBJECTIVES
SUB-COMMITTEE

LONDON—H.M. STATIONERY OFFICE

OFFICE OF MILITARY GOVERNMENT FOR GERMANY (US)
FIELD INFORMATION AGENCY, TECHNICAL

FIAT FINAL REPORT NO. 610

21 March 1946

DIMENSIONING OF DIRECTIONAL ANTENNAS
According to Dr. Kurt Fränz

BY

A. M. STEVENS

Joint Intelligence Objectives Agency

FIELD INFORMATION AGENCY, TECHNICAL

A B S T R A C T

A translation of a paper covering a resume of the basic dimensioning of directional antennas developed in the last few years by Telefunken as written by a physicist and engineer of the Telefunken laboratories. 39 pages including 16 pages of figures and diagram.

REVIEW OF THE BASIC GROUNDWORK FOR THE DIMENSIONING OF DIRECTIONAL ANTENNAS

by

Dr. Kurt Fränz

of

Telefunken G.m.b.H., Berlin
No. 8 Max Strasse

Contents:

This paper covers a resume of the basic dimensioning of directional antennas which in the last few years have been developed by Telefunken G.m.b.H.

A print of the original German text has been sent to the Joint Intelligence Objectives Agency in Washington.

Berlin, Schöneberg, October 27th, 1945.

Dr. Kurt Fränz
Physicist and Engineer for
Telefunken Laboratories.

SECTION I

ANTENNAS AND RANGES

By directional action of transmitting and receiving antennas it is possible to increase the gain as compared to a single dipole. The gain in performance by grouping as compared to the elementary dipole is the "gain"of the antenna. In place of this "gain" it is also possible to make use of the effective surface of the antenna which frequently makes the essential relationship appear more clearly.

As is known, the gain "g" is related to the shape of the field strength diagram $E(\vartheta, \varphi)$ and permits us to calculate it by means of the integration of the diagram

$$g^{-1} = \frac{3\pi}{8} \int \frac{E^2}{E_0^2} \, d\Omega \qquad (1)$$

E_0 is the field strength in the direction of the transmitter-receiver, ϑ and φ are width and length coordinates of a spatial coordinate system and $d\Omega = \cos\vartheta \, d\vartheta \, d\varphi$ is the differential of a spatial angle. (When speaking of "gain" as such without reference to a particular direction, the maximum value of the gain is always meant.)

In the era of the short wave directional antenna for transoceanic service the gain was very suitable for estimating the effect of stacking or grouping on the energy transmission; as is discussed in greater detail below, the gain is equal to approximately 1 in the case of the usual dipole antenna. The concept of the antenna effective surface F is adapted to the newer antennas such as parabolic mirrors, horn antennas, slit tubular radiators, etc., which are preferred in the decimeter and centimeter technique. It (F) is correlated with the gain "g" by the Formula

$$F = \frac{3}{8\pi} \lambda^2 g \qquad (2)$$

In the receiving case one can define the effective area also as that area through which a plane wave transports just as much power as the maximum which can be withdrawn from it by the antenna; namely, by impedance matching. Therefore we frequently speak of "absorption" surface rather than "effective" surface.

The effective surface is frequently related to the geometric antenna surface in a very simple manner. In the case of a Telefunken Tannenbaum antenna, which is the most frequently used multiple in Germany, the effective surface is exactly equal to the rectangular geometrical surface of the antenna. The relation between

the effective surface F_w and the geometrical area F_{geom} is called the surface usability or efficiency of the antenna and is considered as a measure of efficiency of the grouping obtained with an antenna of a given geometrical surface. With the concept of effective surface it is possible to obtain a practical simple beam width formula.

For the energy balance of wireless transmission through space, for example, the following formula is found

References 14, 15, 16. $$N_e = N_s \frac{F_s F_e}{r^2 \lambda^2} \qquad (3)$$

N_e is the received power, N_s the radiated power, F_s the effective surface of the transmitting antenna, F_e that of the receiving antenna, r the distance between transmitter and receiver and λ the wavelength. It is obviously necessary that the engineer set up rules for dimensioning antennas which are sufficiently real to be usable in practice. It is shown that for the effective surfaces of antennas which are large in terms of wavelength limiting laws of the desired simplicity are valid. Sharply bunching antennas which are of special interest today are the large antennas, and moreover, it has been found that the limiting laws which are strictly valid in the case of large antennas are valid practically even in the case of very small antennas. We have therefore set up the limiting laws for effective surfaces and gains of our common antenna types.

SECTION 11

DIPOLE DIRECTIONAL ANTENNAS

In the case of a large Telefunken Tannenbaum antenna (see Fig. 1) the effective surface is equal to the geometrical antenna surface. The gain per half wave dipole, in practice, is taken as 1; with this rule it is not important whether or not the dipoles are fed or only radiation coupled. The gain of 1 per dipole would in fact be expected if the radiation resistance of the dipoles connected to the antenna were not appreciably altered from the value of 73 ohms for a single dipole. In reality the dipoles have partly larger, partly smaller radiation resistances than 73 ohms (Ref. 42) and only in the middle of all dipoles the radiation resistance remains unchanged (Fig. 2). Exact calculation shows that for the radiation in the case of a Tannenbaum antenna consisting of four dipoles the gain per dipole is equal to one within a few percent. In the case of this kind it is not important that the antenna be square. Appreciable deviating values shown are valid only for horizontal and vertical dipole arrays in which all of the dipoles are arranged in the same straight lines either in the direction of polarization or normally thereto (Fig. 3). In a horizontal dipole array of N dipoles with the usual distance of a half wavelength between neighboring dipoles ($d = \lambda/2$) the following is valid

$$g = \frac{4}{3} N \tag{4}$$

Refs. 35, 8, 9. For corresponding vertical dipole array the following equation is valid:

$$g = \frac{2}{3} N \tag{5}$$

As long as the distance d between neighboring dipoles is small in comparison with one wavelength, it is true that the gain depends only on the length $b = Nd$ of the antenna, but not upon the density of the loading with the dipoles. The gain per dipole is represented in Fig. 4 as a function of d/λ for vertical and horizontal arrays. When antennas are arranged in an antenna group, for example, as in the above mentioned arrays, it is known that a polar diagram results which is formed by multiplication of the single antenna diagrams by a diagram according to the group arrangement. When the distance between neighboring dipoles in horizontal and vertical dipole arrays is selected as equal to one wavelength there is formed an auxiliary maximum in the group diagram which attains the magnitude of the main maximum. In the case of a vertical dipole array a zero point of the dipole diagram is located exactly in the antenna direction in which the new high maximum of the group diagram which attains the magnitude of the main maximum. In the case of a vertical dipole array a zero point of the dipole diagram is located exactly in the antenna direction in which the new high maximum of the group

diagram is located, but in the case of a horizontal dipole array this is not the case and this explains the difference between the two curves of Fig. 4. The irregularities in the curves in Fig. 4 appear only in the limiting condition of infinitely wide antennas; for finite antennas the true curve deviates from the limiting curve in the immediate vicinity of the irregular intervals in such a manner that they are regular everywhere.

Apart from these irregular intervals the values for finite antennas differ but little from those in the curves in Fig. 4. This is shown by Fig. 5 in which the gain per unit figure of the antenna is represented as a function of the antenna width for horizontal and vertical arrays with uniform current loading. The usability of the limiting laws for rather small antennas is also evident by incorporating in the limiting laws for very large horizontal and vertical arrays, with the usual distance $a = \lambda/2$ between neighboring dipoles, the next term of an asymptotic series progressing by negative powers of N,

$$\left(\frac{g}{N}\right)^{-1} = \frac{\pi}{4} + \frac{3\ln 2}{\pi^2 N} + \cdots\cdots = \frac{\pi}{4} + \frac{2}{N} + \cdots\cdots \qquad \text{(Horizontal)}$$

$$\left(\frac{g}{N}\right)^{-1} = \frac{\pi}{2} - \frac{6\ln 2}{\pi^2 N} + \cdots\cdots = \frac{\pi}{2} - \frac{\ln 2}{N} + \cdots\cdots \qquad \text{(Vertical)}$$

In a horizontal dipole array where $a = \lambda/2$ it is not necessary, as in the preceding examples, to feed all dipoles in phase, but it is possible instead to feed alternate dipoles out of phase. Then, as is shown in Fig. 6, the main maximum is no longer normal to the plane of the antenna but lies in the same plane as the antenna; in this case there is obtained the same gain as is obtained with the vertical dipole of equal width.

$$g = \frac{2}{3}N \qquad (6)$$

Up to this point we have considered dipole antennas in which currents of equal amplitude flow in all dipoles. In order to obtain smaller secondary maxima than result from the assumption, use is made of antennas, the excitation of which is in phase but decreases in amplitude from the center to the edges. In comparison with an equally large antenna which is excited not only in phase but also with uniform amplitude, there results a diminution of effective surface which can be easily calculated from a distribution of excitation amplitude J over the antenna surface. The effective surface is, namely,

$$F = \frac{\left(\int J\,dl\right)^2}{\int J^2\,dl}; \qquad (7)$$

where ds is the surface element of the antenna and the integration is to extend over the entire antenna; if the loading is not uniform but consists of single dipoles whose distance from one another is smaller than one wavelength, then Equation 7 is modified by substituting for the true discontinuous loading a uniform loading averaged over sections of one half wavelength. In the derivation of Equation 7, there is further assumed a unilateral radiation diagram which is produced in the case of the Tannenbaum antenna by the reflector walls. In the case of large antennas, in order to calculate surface efficiency, it is therefore not necessary to first determine the diagram from the current loading and from that the gain from Equation 1. It is much simpler to calculate directly from Equation 7 the gain or the effective surface from the loading (Refs. 1, 2, 3). For example, assuming with Barrow and Chu that in a sector beam of rectangular cross section which is excited by an H wave there exists a sinusoidal distribution along one cross-sectional side and a uniform one exists along the other cross-sectional side, then there results for horns which are not too small a surface efficiency of 0.81.

It should be once more emphasized that if nothing else is said the rules for effective area and gain are the limiting laws for antennas which are large in terms of wavelength.

If the assumption is omitted that all the antenna elements are excited in phase the effective area can in principle theoretically become much greater than the geometric surface. Ref. 11. By analogy with multi-pole radiators of optics it is even possible to design antennas which, with relatively small dimensions and with bunching of any needed sharpness, possess effective surfaces which will be as large as desired. However, antennas whose effective surfaces are substantially greater than their geometrical surfaces possess so extremely small radiation resistance that the transmitter power is converted only into heat, so that, in spite of their great gain, these antennas are not usable. For example, there exists no favorable current distribution on vertical antenna wires which would lead to maximum gain with a given antenna height and wavelength and this in spite of the fact that the literature occasionally describes such antennas. (Ref. 28)

The dipole antennas employed in practice are in most cases transverse radiators; that is, the main maximum of the radiation diagram is normal to the antennas; in general, in this case what is desired is uniformly strong and uniformly phased excitation of all dipoles.

In this case a very definite type of diagram is obtained which is essentially represented by $\frac{\sin x}{x}$, for example, in a

horizontal array

$$\frac{\sin\left(\frac{N\pi d}{\lambda}\sin\varphi\cos\vartheta\right)}{\sin\left(\frac{\pi d}{\lambda}\sin\varphi\cos\vartheta\right)}\cos\vartheta \qquad (8)$$

The first auxiliary maximum attains 0.22, the second 0.11 of the value of the main maximum. Between the antenna width $b = Nd$ and the two first null points to the right and left of the main maximum lies the zero value angle 2ε

$$2\varepsilon = 120^\circ\frac{\lambda}{b} \qquad (9)$$

A type of diagram materially different from the above is obtained by alternate counter phase feeding of the dipole.

$$\frac{\sin\left(\frac{N\pi}{\lambda}\sin\varphi\cos\vartheta+\frac{n\pi}{2}\right)}{\sin\left(\frac{\pi d}{\lambda}\sin\varphi\cos\vartheta+\frac{\pi}{2}\right)}\cos\vartheta \qquad (10)$$

If we assume at first $d = \lambda/2$, this diagram is of the type of $\frac{\sin\chi^2}{\chi^2}$ the maximum lies in the longitudinal direction of the antenna. In the case of the zero angle 2ε the following equation is valid

$$2\varepsilon = 230^\circ N^{-\frac{1}{2}} = 163^\circ\left(\frac{\lambda}{b}\right)^{1/2} \qquad (11)$$

If $d < \lambda/2$ there is obtained instead the general diagram type

$$\frac{\sin\frac{k\pi}{\lambda}(\chi^2+a)}{\frac{k\pi}{\lambda}(\chi^2+a)}$$

Where

$$a = \frac{\lambda}{2d} - 1 \qquad (12)$$

The effective area increases with the increase of auxiliary lobes, if, while maintaining a fixed antenna length b the distances between neighboring dipoles are reduced toward a half wavelength. This was first pointed out by Zinke (Ref. 40). The two effects are shown in Fig. 7. In this case the main maximum no longer necessarily lies in the longitudinal plane of the antenna. The diagram of the di-electric antenna described in detail below, shows a close correspondence with those treated

by Formula 12.

It is known from numerous measurements and especially by calculation that non-uniform excitation of an antenna leads to smaller auxiliary lobes than uniform excitation, provided that the center is excited more than the edges. It is frequently pointed out that in the case of dipole antennas a distribution of excitation according to binomial coefficient leads to a diagram without auxiliary maxima

$$\cos^n\left(\frac{\pi}{2}\sin\varphi\cos\vartheta\right)\cos\vartheta \qquad (13)$$

Apart from the very poor surface utilization in large antennas (n very much greater than 1) it is not easily possible to create non-uniform leading of dipole antennas, especially in the case of relatively wide frequency bands. On the other hand the parabolic mirrors and horn radiators described in greater detail below present non-uniform loading with simultaneous convenient feeding. They are therefore much more suitable for the production of diagrams with small auxiliary lobes than are dipole antennas.

If it is desired to employ antennas, in which it is intended to excite all dipoles in phase, for the production of broad frequency bands. the wide frequency character of the diagrams can be obtained without difficulty by the employment of equally long feed lines for all dipoles; on the other hand it is more difficult to obtain wide band characteristics by matching the antenna to the feeding cable. Very high requirements for the precision of matching must be fulfilled particularly in television. where reflections of a plurality of images are displaced from one another by the transmission time through the cable; also in the case of self excited transmitters there appear alternate frequency variations caused by the balancing and unbalancing influences of inadequate matching. these phenomena being observed the more easily the greater the mis-matching and the longer the cable between the transmitter and the antenna. The transmission band of one single dipole widens with the thickness of the dipole. According to calculations by Schlayer. the band width of a single dipole can be approximately doubled by radiation coupling. while with several radiation coupled dipoles it is possible to obtain about 3 times the width of a single band beam. Concerning compensation and transformation connections greater details are given below.

With dipole antennas which are intended to produce only a single maximum it has been possible heretofore, in all cases, to obtain adequate wide beam properties of diagrams and impedances. While with cross bearing with two alternate connected diagrams this procedure did not always lead to the desired results.

SECTION III

PARABOLIC ANTENNAS

For the production of very sharp multisided bunching the radially symmetrical parabolic mirror is especially suitable because it requires only a single fed antenna.

The surface efficiency of the parabolic mirror is smaller than 1 for three reasons. that is, the effective surface is smaller than the aperture of the mirror. Reference 18. If there is used as a radiator near the focus a fed dipole with a radiation coupled reflector, then the surface efficiency is 0.65 at most. This is so because first of all only a part of the radiation sent out by the dipole radiation falls upon the mirror, the fraction with optimum dimensions being 0.78; secondly the excitation of the mirror is non-uniform, in the center of the mirror aperture the higher radiation density exists and this as compared with uniform excitation leads not only to smaller auxiliary lobes in the radiation diagram, but also to reduction of the effective surface. Thirdly, the prolongation of the radiation entering the orifice is parallel to that of the dipole, only in the two mutually normal symmetrical planes determined by the dipole the radiation of the dipole also prevailing in a distant up-stream point of the mirror axis.

The falsely polarized component contributes to the distant diagram only outside the mirror axis and this results in an efficiency diminution of the effective surface. The two last named defects explain the difference between the two values 0.65 and 0.78 above.

The most favorable dimensions of the mirror, with the prebunching attainable by means of the dipole reflector combination requires a mirror diameter ratio to focal length of $2\sqrt{2}$. As shown in Fig. 8 it is not necessary to maintain their values with very great precision. If flatter mirrors are used it is true that only a small fraction of the radiation power falls upon the mirror. On the other hand the coverage (illumination) is more uniform and the falsely polarized component is weaker; conditions are then approached which prevail with a plane mirror. If more highly curved mirrors are used a larger fraction of the radiation power will fall upon the mirror but its coverage becomes poorer.

If sharper prebunching than is obtainable with the dipole and reflector, particularly also diagrams approaching conical shapes more closely than is the case in the above arrangement then it is possible expediently to use even flatter mirrors and surface efficiencies are obtained which lie 0.65 and 1.0.

If the prebunching is accomplished not by the above arrangement but, for example, by means of a horn radiator, the question arises of how the mirror should be located with respect to the prebunching diagram and how sharp this diagram should be chosen. If it is made too sharp it is true that almost all the total radiated power strikes the mirror but the coverage is not uniform. If too slight prebunching is chosen these conditions are reversed. As a rule for the selection of prebunching, it is well to remember that the mirror aperture, vertical to the plane of prolongation, must intersect the prebunching diagram at an angle at which the power amounts to approximately 35% of maximum. (Fig. 9).

The effective surface is quite insensitive toward defocusing of radiation, as introduced for the purpose of diagram control of focus.

If there exists only one dipole and reflection is neglected, the best surface efficiency is 0.375; the corresponding depth of mirror, as measured by diameter to focal length ratio is equal to 4, and the focus lies exactly in the plane of the mirror aperture which is already known from a work by Darbord (Ref. 6).

All of these statements are again valid as limiting laws for large mirrors or reflectors.

In the case of very flat parabolas of uniform coverage density there are obtained the diagrams known from optics and corresponding to circular shaped type $2J_1(x)_x$ where J_1 is the Bessel function of the first order. The first auxiliary maximum is smaller than in the case of the rectangular Tannenbaum antenna and amounts to only 0.13 of the value of the main maximum (Ref.19). The diagram is somewhat wider than in the case of a horizontal array whose length is equal to the mirror diameter. Both diagrams are represented in Fig. 10. The diagrams which are obtained for various mirror depths, when only a dipole without a reflector is in the focus, are represented in Figs. 11 and 12. In the equatorial diagram normal to the plane of polarization, deviations appear only in the case of very deep mirrors and these consist of relatively small auxiliary lobes of, for example, 5%, with a mirror parameter $q = 0.5$

$$q = \left(\frac{4 \times \text{mirror aperture}}{\text{mirror diameter}}\right)^2$$

In a meridional diagram auxiliary lobes of less than 10% are obtained.

The possibility of modifying diagrams by radial defocusing is frequently of interest. With very flat mirrors the diagram is displace by the same angle by which the dipole is defocused, corresponding to a

reflection of light waves from a plane mirror. With deeper mirrors the diagram displacement lags behind this angle by the function of $\frac{1}{2(1+q)}$; this formula, however, is not valid in the case of very large defocusing. The auxiliary lobe located in the side of the mirror axis increases rapidly during radial defocusing. This aberration is known in optics as "KOMA". The disturbing auxiliary lobe becomes smaller, the flatter the mirror. For reflection from plane mirrors, the whole diagram is displaced by the angle of reflection while preserving its original form including the height of the auxiliary lobe. Moreover, the disturbing auxiliary lobe is smaller when defocused in the meridional plane than in the equatorial plane. It is recommended to make the mirror as flat as is possible without reducing the efficiency and without inconveniently great focal length, and to select $q = 3$. Figures 13 and 14 represent 2 diagrams which are obtained by prebunching with a dipole, with a radiation coupled reflector, q being equal to 3, a radiation displacement of 3^0 being used and a mirror of 80 wavelengths diameter being employed; the two figures represent the two defocusing possibilities discussed above. In the case of the more favorable defocusing in the polarization plane the auxiliary lobe attains only a value of 20%.

The reaction of the mirror upon the impedance of a dipole in the vicinity of the focus is expressed by

$$\frac{R}{R_0} = 1 - 3\gamma \cdot \frac{e^{-\gamma K p}}{K_p} \qquad (14)$$

where R_0 = resistance without mirror

$K = \frac{2\pi}{\lambda}$ $\qquad$ P = 2 x aperture

With large mirros the diagram and the impedance both possess a broad band characteristic.

SECTION IV

SLIT RADIATORS

Slit radiators were first developed by Muth of Telefunken and Gebau of the University of Jena. When sharp bunching is desired in one plane only and a substantially less bunching is desired normally to the plane, it is possible to employ cylindrical parabolas which are excited along their focal axis. The length L of the focal axis determines the sharpness of the diagram in the plane of stronger bunching, while the angle of the aperture in a plane normal to the focal axis determines the sharpness in this plane. A relatively simple feeding of the antenna is arrived at by using in the focus a unilaterally fed longitudinal slotted tubular conductor.

which has its slot and therefore itsradiation turned towards the parabole, from which the radiation is reflected. There is excited in the tubular conductor a progressive H_1 wave, whose polarization is vertical to the slot. If the tubular conductor could be excited exactly with its limiting wave λ_g , then the field along the entire slot would be in phase, and therefore the maximum of the radiation would lie normal to the aperture surface of the cylindrical parabola. In practice, it will be more expedient to select a wavelength $\lambda < \lambda_g$, which is propagated along the tube with the phase velocity

$$V = \frac{c}{\sqrt{1-\left(\frac{\lambda}{\lambda_g}\right)^2}} \qquad (15)$$

where C = the velocity of light.
(Only approximate because of the slot.) While the shape of the diagram is maintained it leads to a diagram displaced by an angle φ from a line normal to the mirror aperture (see Diagram 15.)

$$\sin\varphi = \frac{c}{V} \qquad (16)$$

(Angles of approximately $\varphi = 30^\circ$ are desirable).

By radiation losses the wave is exponentially damped as it progresses along the slot. The height of the slot determines the damping constant β By making the total damping small $\beta L \ll 1$, it is possible to attain a condition under which the progressive wave has nearly the same amplitude at the far end of the tube as at the fed end. If the wave is absorbed in an impedance it is true that the coverage of the parabola becomes uniform and the gain is a maximum but the efficiency is poor. If the wave is allowed to be reflected from the far end, then a second strong maximum is obtained in the polar diagram under the angle $-\varphi$, and the power arriving at the far end goes over into this undesirable maximum, and must also be considered as a loss. If the total damping is made large, $\beta > 1$, then the entire power is radiated off through the slot and contributes to a single main maximum; due to the non-uniform excitation, however, the "gain" is now too small. The product of surface utilization and efficiency must therefore reach its maximum when the focal damping is of medium degree βL

is approximately equal to 1) and this product is materially smaller than its theoretically maximum value of 1. With more precise calculation, there is obtained for any desired length L of the focal axis, the most favorable total damping $\beta L = 1.3$ so that, with the best dimensioning

the amplitudes of the progressive wave have fallen off at the far end by 30%. The product of efficiency and surface utilization attain then the value of 0.81 so that it does not pay to employ irregular slots widened toward the far end, as has been occasionally attempted, in order to approximate values of Fig. 1. Fig. 16 shows that it is not important to maintain precisely the value $\beta = 1.3$. An approximation of the relationship between damping and slot width with rectangular and circular cross-sections of tubes is given by the following formulas.

$$\beta L = \frac{\pi \cos^2 \varphi L h^2}{4 \sin \varphi \lambda F} \quad \text{(Rectangles)} \qquad (17a)$$

$$\beta L = 2.17 \frac{\pi}{4} \frac{\cos^2 \varphi L b^2}{\sin \varphi \lambda F} \quad \text{(circles)} \qquad (17b)$$

F = area of the tube cross-section
h = slot width

These formulas are obtained by assuming that the current distribution in the tube is not disturbed by the slot, except for the energy lost through the slot. In reality the radiation loss depends upon the current distribution, especially on the outside of the tube; the true damping should be somewhat greater than shown by the above formulas. Until the end of the war, however, there had been no experimental work done showing the relationship between the slot dimensions and the damping, nor, any adequate experiments for determining the most favorable slot width.

For the diagram for the slotted radiator, there is obtained the following formula.

$$E^2 = \frac{\alpha (\beta L - \cos(KL \sin\alpha))}{(\beta L)^2 + (KL \sin\alpha)^2} \qquad (18)$$

Where $K = 2\pi/\lambda$ (number of waves)

α = the angle calculated from the direction of the maximum.

For long slots, there are obtained slot widths "h" of a few millimeters which are difficult to maintain, easily clog up under the influence of weather and offer poor insulation. These disadvantages can be avoided by replacing the narrow slot and using one side of a rectangular tube or a grid (Ref. 20), and the damping constant in this case can be calculated from

the width and spacing of the elements, similarly as in the case deflection grids, which are hit by a plane wave at an angle φ

SECTION V

DI-ELECTRIC ANTENNAS

See References 30 and 38

The di-electric antennas were developed by Mallach, Wegener and Zinke in the Heinrich Hertz Institute. The following presents the results of their researches.

Di-electric antennas consist of slightly conical rods of circular or rectangular cross-section made of di-electric materials, one end of which is closed by a metallic surface as a reflector, an exciting dipole being imbedded into the di-electric in front of the metal surface.

In an infinitely long di-electric rod energy can be propagated without lateral radiation loss, exactly as in a closed hollow metal tube. This is illustrated most simply by the example of an infinitely extended di-electric located between two parallel planes; between the limiting planes of the di-electric a plane wave can be propagated by total reflection in a zig-zag path without modulation provided that the wave hits the limiting planes at a sufficiently small angle. See Refs. 32 and Fig. 17. If we designate the angle of incidence, as the angle between the plane normal to the ware and the plane normal to the limiting plane as φ then the sine of this angle must, as is well known, be greater than the reciprocal of the index of refraction,

$n = \sqrt{\varepsilon}$ of the di-electric.

$$\sin\varphi > \frac{1}{n} \qquad (19)$$

Outside the di-electric the field decreases exponentially with decreasing distance Z from the limiting plane, the decrease being proportional to

$$e^{-\frac{2\pi z}{\lambda}\sqrt{\varepsilon \sin^2\varphi - 1}} \qquad (20)$$

The flatter therefore the incidence the greater φ the more rapidly is the decrease of the field, and the more does the field remain confined to the interior of the di-electric and to its immediate vicinity.

Exactly as in the case of a metal tube of rectangular cross-section, there results in the medium, due to superposition of the fields reflected from the two limiting planes, a wave, which progresses along the limiting plane with the phase velocity,

$$V = \frac{c}{n \sin \varphi} \qquad (21)$$

When the angle of incidence decreases from 90^0 to the limiting angle of total reflection, the phase velocity increases exactly from the value of $\frac{c}{n}$ for infinite thickness of di-electric, to the value of the velocity light in vacuum C. The relationship between V and the layer thickness is easily calculated from the limiting conditions for the electromagnetic field at the limiting planes and it has been found that $V = \frac{c}{n}$ for infinitely thick layers and $V = C$ for an infinitely thin layer as had been first predicted. A proper limiting wave as it exists in hollow metal conductors, does not exist in this case. In round rods the relationship among phase velocity, di-electric constants and rod diameters has been calculated in principle by Hondros and numerically by Wegener (see Refs. 23 and 38). The values obtained by the latter, which correspond well with the measurements of Mallach, are reproduced in Fig. 18. They refer to the simplest wave type which can be excited with a dipole; in the terminology obtained from theory for hollow conductors, this wave type corresponds to the superposition of an H_1 and an E_1 wave, which, in contrast to a hollow conductor, are in this case not capable of separate existence.

A rod of finite length radiates spherical waves, its polar diagram largely corresponds to that of a horizontal dipole slot with alternately counter phase feeding of the dipoles; except that the distance between neighboring dipoles is not equal to $\frac{1}{2}$ the vacuum wave length but is diminished by the factor $\frac{V}{C}$. They have therefore been already discussed in the section on dipole antennas.

$$\frac{\sin \frac{\pi L}{\lambda}\left(\cos\psi \cos\vartheta - \frac{c}{V}\right)}{\frac{\pi L}{\lambda}\left(\cos\psi \cos\vartheta - \frac{c}{V}\right)} \cos\vartheta \qquad (22)$$

The azimuth ψ is here calculated from the rod axis in order that a maximum takes place in the direction of the rod axis $\psi = 0$ and

$$\frac{L}{\lambda} \ll \left(\frac{c}{V} - 1\right)^{-1} \qquad (23)$$

must obviously be valid, that is, the longer the antenna, the sharper therefore the bundling, the less must the phase velocity differ from thevelocity of light and the smaller also the conduction o the field through the rod as exemplified by the plane problem discussed above. Morecover, the numerical results of Wegener show that with large di-electric constants the phase velocity is even constant only in a relatively narrow wave band. Therefore di-electric wave antennas have been predominately constructed of materials possessing the rather low di-electric constant of $\varepsilon = 2.5$ (Trolitul). According to experience when such a di-electric constant is used the cross-section of the rods must be greater than $.1\lambda^2(\varepsilon-1)^{-1}$ in order that the propogation of the wave may still take place.

It has been further found that the rods must be of a slight conical shape, because otherwise there appears at the end which is not fed a considerable wave reflection which results in strong auxiliary lobes and reflected radiation. MaTlock and Zinke recommend that the cross section be reduced from .25 to $.1\lambda^2(\varepsilon-1)^{-1}$ In that case, according to Malloch, the measured diagrams correspond well with those derived from Formula 22 which are calculated under the assumption that only a progressive wave, not a reflected wave, exists. According to the calculations of Wegener, angles of loss of the di-electric may reach 5% without resulting in poor efficiency.

In place of a solid rod it is also possible to make use of thin walled cylinders. According to practice the diameter of the cylinder must lie between 1 and just over $\frac{1}{2}$ vacuum wave length, and must therefore be greater than in the case of the solid material; the wall thickness must amount to approximately $.1\lambda^2(\varepsilon-1)^{-1}$

It is true that greater bunching is difficult to accomplish with one single radiator; however, di-electric radiators as in the case with dipole can be connected into groups; in this case, on account of the stronger bunching of the single element, the distance between neighboring elements can be greater than in the case of dipoles.

SECTION VI

HORN RADIATORS

See Refs. 1, 2, 3, 26, 27, 34, 36, 37.

Horn Radiators are particularly suitable for connection to concentric lines. As is known they do not make it possible to secure as much bunching as might be desired and this is directly obvious by considering the limiting case of optics. The literature shows unanimity concerning their dimensioning

but not concerning the surface efficiency attainable by their use. A summary of the various published measured values in Fig. 21 shows large discrepancies. A measuring process, described further later on, for the direct measurement of absorption surfaces has not net been applied to horn radiators. Since the coverage of horn radiators is rather non-uniform, values of less than one should be expected for surface efficiency even the case of moderately large horn radiators.

In order to obtain sharper bunching Telefunken used horn radiators for the excitation of parabolas while Blaupunkt connected horn radiators in parallel arrays.

SECTION VII

ANTENNA MEASUREMENTS

Polar diagram measurements were carried out with apparatus of largely automatic action. The antenna to be measured was mounted as a transmitting antenna on a rotating frame which was driven by a synchronous motor with constant angular velocity.

A receiver equipped for registering the diagram was set up at a sufficiently great distance ($d \gg \frac{b^2}{\lambda}$ where d = distance, b = antenna width). The receiver was likewise equipped with a directional antenna which was intended to reduce the influence of undesirable reflections. In order to avoid reflections from the ground the antennas were set up, for example, on the roof of two opposite wings of a 'U' shaped building. When it was desired to observe for auxiliary lobes down to 5% of the main maximum, the receiver was equipped with a square law detector with a low frequency amplifier; the registration of smaller auxiliary lobes was effected by a receiver using linear detection. The diagrams were generally drawn by logarithmic recorders (Neumann-Recorders), which possessed an adjustable steady speed. Simultaneously angular marks were electrically transmitted from the rotating frame to the recorder. With such an arrangement, amplitude ratios of 1000 to 1 could be easily detected.

Measurements of gain or surface efficiency can be replaced only with difficulty by measurements of the diagrams. It is of course possible to take the total spatial diagrams and to calculate therefrom the gain by numerical integration; this process however, is so complicated that it can be used only infrequently in practice when the diagrams of an antenna type and the corresponding surface efficiency are as precisely known as those of a dipole antenna, in which case it is sufficient to check the diagram in one or two mutually normal surfaces and, if it agrees with expectations, to assume that it also agrees in the intermediate directions

and therefore possesses the estimated effective surface. In general, however, measurements of the diagram in two planes is not sufficient. For example, in the case of a large square Tannenbaum antenna, the diagram is identical in the two planes parallel to the sides of the square. If, unaware of the true situation, one should attempt to complete the diagram in the intermediate direction by assuming it to be radially symmetrical--while in reality it is so only in the region of the main lobe--then the error could be extremely large with increasing bunching. In this case, too much radiation is assumed to exist outside the main lobe. and it is found, for example, with a side length of a Tannenbaum antenna equal to 10 λ that the surface efficiency is 0.58 instead of the true value of 1. The sharper the bunching the more precisely (that is, down to smaller absolute values) would it be necessary to measure the auxiliary lobes, because the main lobe then occupies only a small faction of the total spatial angle of 4 π

As is known a comparison of the effective surfaces of two different antennas requires only the easily excited relative measurement of two voltages. As normal radiators of known effective surface, dipoles are employed for longer waves; in the case of decimeter and centimeter waves, however, it is not possible to obtain a dipole diagram due to the influence of the instrument upon the diagram, Ref. 12. What, however, is less generally known, is that by means of a relative measurement of two voltages it is possible to carry out an absolute measurement of any desired antenna. The principle is illustrated in Fig. 19 . In the simplest case two identical antennas are taken. One of these is matched to a transmitter of internal impedance, for example, Z = 70 ohms; the other is matched now to an ohmic resistance, also of 70 ohms. The voltage u formed at the resistance is determined relatively to the voltage u_o , which is found when the transmitter and resistance are coupled directly without the wireless connection by way of the two antennas. If r is the distance between the antennas and λ the wavelength, then the effective surface is expressed by

$$F = r\lambda\sqrt{\frac{u}{u_o}} \qquad (24)$$

The relative measurements of the voltages is most precise when a superheterodyne receiver is used and the output voltage of the receiver produced by the two input voltages u and u_o are reproduced with an intermediate frequency measuring transmitter. The voltage ratio $\frac{u}{u_o}$ can then be read off from the voltage divider of the measuring transmitter. In this procedure the requirements for precision matching are less.

The measurements of antenna impedances were carried out with straight concentric lines when high precision was required; with good measuring lines (Lotos) a measuring precision of 1% could be obtained. These lines contained interior leads of ground silvered ceramic tubes which sagged only little

under their own weight, and were supported only at the two ends of the measuring lead-in insulated supports. These supports were constructed in such a way that they caused no mismatching. The deviation, caused by the longitudinal slit of the measuring lead, from the characteristic impedance of the corresponding concentric cable, was determined by the Meinke node displacement method (Ref. 31). In this method, use is made of a geometrically precise concentric line of variable length, which is shorted on one end, is connected to the measuring lead in the other end and has no slit itself, but is otherwise in exact correspondence with the dimensions of the measuring line; this arrangement was used as a resistance standard and more particularly as a reactance standard. If the measuring line had exactly the same characteristic impedance as the unslotted line, then the node displacement in the measuring line would be equal to the length of the connecting reactance. From the variation of the node displacement from exact proportionality with the reactance length it is possibl to determine with great precision the small change in the characteristic impedance of the measuring lead caused by the slit.

For the measurement of an impedance with regard to amplitude and phase it is necessary, with a stretched line, to take account of the current distribution in the line by means of a somewhat time consuming measurement. Since this usually takes too much time with antenna matching, Schmid developed a circular wound measuring lead (AURORA) with a steadily rotating brush (SONDE) (50 cycles) with which the current distribution in the line is made visible as a stationary image on a Braun tube. With this it is possible to undertake rapid adjustments of antenna tuning, transformation, etc.

If it is desired to indicate the amount of mismatching and not the phase relation it is possible to employ simple direct indicating bridge arrangements according to Buschbeck and Paul. The voltage between points 1 and 2 of the bridge arrangements drawn in Fig. 20 is given by

$$M_{1,2} = \left| \frac{Z-R}{Z+R} \right| V \qquad (25)$$

and is therefore only a function of the mismatching; with constant input voltage V the bridge instrument can be calibrated directly while mismatched. Similar bridges can also be arranged with good precision in the decimeter region, (KALLA).

SECTION VIII

MATCHING PROBLEMS

Relatively complete information is available for the feeding of dipoles. The necessity for matching, as is known, is based on the fact

that the antenna impedance must be transformed by a loss free coupling to the impedance of the feeding cable; at the same time this circuit transforms the specific impedance into the complex conjugate of the antenna impedance. Although the problem is solvable for all fixed frequencies. It cannot in principle be solved for frequency bands of any desired width. The existance of the theoretical limit is formed from an extension of the Foster reactance theorem to cover any desired impedance, Refs. 13 and 16. The rate of change of the reactance is fairly definitely fixed by the change of the effective resistance as a function of frequency. If the antenna impedance is approximately represented by a series or parallel resonant circuit—this corresponds to the current resonance of the centrally fed half wave dipole, or, to the voltage resonance of the centrally fed full wave dipole—, and if the equivalent circle diagram has the damping d, then, no matter how many loss free connections are employed, a matching is possible only in the frequency interval shown in the following formula:

$$\frac{\omega_{max} - \omega_{min}}{\omega_{max} + \omega_{min}} < \frac{d}{\pi} \qquad (26)$$

corresponding limits can also be derived in the case of more complex frequency relationships of antenna impedance.

It is therefore important in the above two significant cases to provide the antenna with as great a damping as possible. For this two methods exist in the case of single dipoles. First, particularly thick radiators are employed; second, the voltage resonance of the full wave dipole provides a higher damping than the current resonance of the half wave dipole. With equal slenderness ratios (the ratio of the total length L to the diameter ϕ) the damping is greater in the case of voltage resonance ($L \sim \lambda$) by a factor approaching 1.5 than in the case of current resonance ($L \sim \lambda/2$). The characteristic data of tubular dipoles in free space are represented in Fig. 22. In the case of current resonance, the radiation resistance is somewhat independent of the slenderness ratio and R is equal to 73 ohms. The damping can be calculated from the resistance and the frequency relationship of the reactance $\frac{\delta X}{\delta \omega}$ and the resonant frequency ω_0 by means of

$$d = \frac{2R}{\omega_0 \left| \frac{\delta X}{\delta \omega} \right|} \qquad (27)$$

and this can be done both in the case of current and voltage resonance.

The relationship in the region of current resonance can be more or less reproduced according to the line theory.

The antenna has a characteristic impedance Z which is given by

(See Ref. 43) $$Z = (120 \ln \frac{L}{\phi} - 66) \text{ ohms} \qquad (28)$$

from which the damping represented in Fig. 22 is calculated from

$$d = \frac{4R}{\pi Z} \text{ (Current resonance)} \qquad (29)$$

For the effective resistance at voltage resonance which depends greatly upon the slenderness ratio $\frac{L}{\phi}$ there is found according to the line theory

$$R = \frac{Z^2}{196} \text{ ohms} \qquad (30)$$

See Refs. 21, 22, 29, 4, 39.

Also in Fig. 22 there are represented values calculated according to the satisfactory Hallen theory.

The values obtained from the line theory agree well with these; yet according to Hallen only rather slender antennas can be thus treated.

Refs. 7, 24, 25, 41.

Both theories agree well with the measured values drawn in. According to the Hallen theory, the antenna damping for voltage resonance has also been calculated (the line theory is of no use here), and these values have been checked by measured values. Moreover, Fig. 23 represents measured shortening factors as a function of slenderness ratio for current and voltage resonance. The shortening factor indicates the amount by which the dipole length L must be shortened in relation to a half wave or a full wave radiator in order that resonance, i.e., disappearance of reactance, may come about.

Actually by coupling the antenna to a simple filter, a half, or better a whole T section in the case of current resonance, or a π section in the case of voltage resonance (Ref. No. 5) the theoretical possible bend width of the antenna is practically achieved. The matching equality resulting therefrom is represented in Figs. 24 and 25.

It is better to use, according to Buschbeck's procedure, dipoles in voltage resonance, in which the longitudinal filter member is constructed as an open quarter wave line in the interior of the tubular dipole. An

example is represented in Fig. 28.

It has been more expedient to employ, as far as possible, assymmetric lines, so that it is necessary to connect a symmetrizing member to the symmetrical antenna. This is shaped either as a loop or as a symmetrizing case, see Fig. 28. Transformation from a fixed ohmic resistance to another ohmic resistance independent of frequency can be theoretically accomplished for any desired band width with loss-free connections and have been carried out in practice up to a frequency ratio of 1:6 so that the limitation of band width could always lie within the antenna, (band width).

See Refs. 24, 7, 35.

In the case of antennas with reflectors and of dipole groups there exists a further method of increasing the band width which was first described by Kauffman. Radiation coupling can be utilized for wide band matching. Distances of $\frac{\lambda}{3}$ between radiator and reflector are recommended. According to calculations of Schlayer the band width of the single dipole can be approximately doubled with a reflector and can be tripled with several dipoles.

In the case of hollow tubes a funnel can be used as an antenna. Problems of matching can, to a great extent, be solved according to the same methods as in the case of concentric lines. In practice when using the relatively narrow frequency bands (with centimeter waves) no great difficulties have been encountered up to the present.

In the case of rotating antennas the transmission of high frequency energy is always effected by capacity coupled collecting rings, which are tightly coupled against undesirable radiation energy losses through joints, either aperiodic by means of high frequency iron or by means of closed cases. The excitation of rotating di-electric antennas, or funnel radiators, is accomplished by means of stationary asymptotic dipoles located in the axis of rotation, these dipoles being constructed as the extensions of the core of the concentric cables.

IX References (Index)

1) Barrow & Greene. Proc. Inst. Rad. Engs. 26 (1938) 1498.
2) Barrow & Lewis. " " " " 27 (1939) 41.
3) Barrow & Chu. " " " " 27 (1939) 51.
4) Bauwkamp. Physics. (1943)
5) Buschbeck. Aus Theorie u. Technik der Antennen 11,72 1943. ZWB.
6) Darbord. L'Onde Electrique. 11 (1932) 53.
7) Dieckmann. (see 5)
8) Franz. Zs. f. Hochfr. 54 (1939).198.
9) Franz. Telefunken-Mitteilungen. 83 (1940) Maiheft.
10) Franz. Zs. f. Hochfr. 59 (1942) 105 u.144.
11) Franz. Zs.f. Hochfr. 61 (1943) 51.
12) Franz. Zs.f. Hochfr. 62 (1943).129.
13) Franz. ENT 20 (1943).113.
14) Franz. Fortschritte der Hochfr. 2 (1943) 685.
15) Franz. (see 5)
16) Franz. (see 5)
17) Franz. E.T.Z. 65 (1944) 229.
18) Franz. Interner Bericht von Telefunken (1944)
19) Franz, Oberhettingen u. Schlayer. Interner Bericht von Telefunken (1944).
20) Goubau u. Mitarbeiter. Interner Bericht des Techn. Phys.Inst.,Jena (1944)
21) Hallen. Upsala Universitets Arskrift (1930).
22) Hallen. Nowa Acta Res. Soc. Scient. Upsaliensis 11 (1938).
23) Hondros. Ann d Phys. 30 (1909) 905.
24) Kaufmann. (see 5)
25) Kotowski u. Schüttlöffel. Aus Theorie u.Tecknik der Antennen 11,64 (1943)
26) Lämmchen. Bericht 137 der Lilienthal-Ges.S.30.(1943). u. Jahrbuch der Luftfahrt-Forschung (1942) S.38.
27) Lämmchen. (see 5)
28) La Paz u Millar. Proc. Inst. Rad. Engs. (1943)
29) Magnus u. Oberhettinger.Zs.f.Hochfr. 57 (1941)
30) Mallach. (see 5)
31) Meinke. Zs.f.hochfr.(1943) u.(1944),ENT (1943 u.1944).
32) Page & Adams. Phys. Rev. 52 (1937).647.
33) Pungs & Lamberts. (see 5)
34) Schäfer. T.F.T.32 (1943) 141.
35) Southworth. Proc. Inst. Rad. Engs. 18 (1930) 1502.
36) Southworth & King. Proc. Inst. Rad. Engs. 27 (1939) S.95.
37) Stutzer. FFO-Buch. (1942), S.93.ZWB.
38) Wegener. Interner Bericht des Heinrich-Hertz-Inst.(1944)
39) Wells. Journal Ins. Electr. Engs. 90 (1943) 143.
40) Zinke. Forschungsbericht 1805 der ZWE (1943)
41) Zinke. (see 5)
42) Bechmann. Zs. f. Hochfr.
43) Brückmann. Antennen. S. Hirzel. Leipzig (1939).

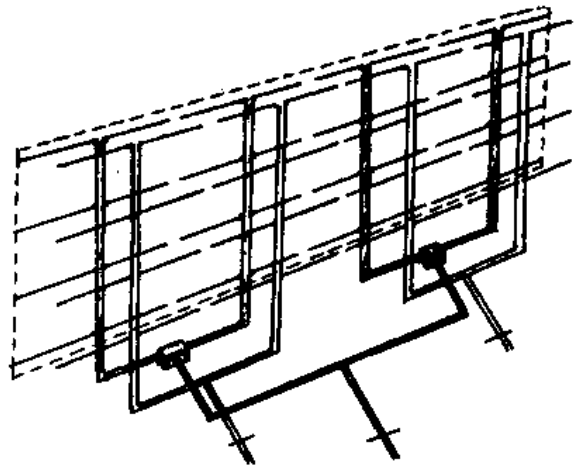

Fig. 1. Telefunken Tannenbaum antenna with reflectors. The geometrical antenna area which is equal to the effective area is shown by dotted lines.

75.4	93	86	86	93	75.4
59.9	67.8	69.9	69.9	67.8	59.9
64	79	74.4	74.4	79	64
64	79	74.4	74.4	79	64
59.9	67.8	69.9	69.9	67.8	59.9
75.4	93	86	86	93	75.4

Each value appears symmetrically four times.

Fig. 2. The distribution of the radiation resistance in a 6x6 half wave dipole array after Bechmann. The dipoles are arranged for direct feeding and are arranged in phase. Average resistance valve is 75 ohms.

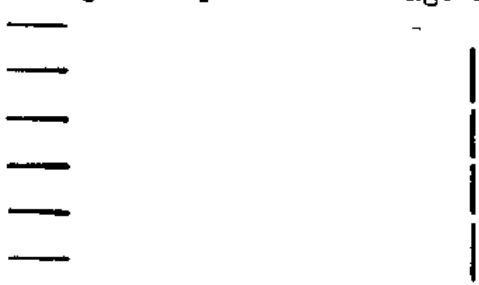

Fig.3 Horizontal dipole array

Vertical dipole array

Fig. 4. Gain per dipole g/n for an infinitely long horizontal dipole array (solid) and vertical dipole array (dotted) as a function of the distance d between neighboring dipoles. The values are valid practically also for the finite antennas except in the immediate surrounding of the spots of irregularity.

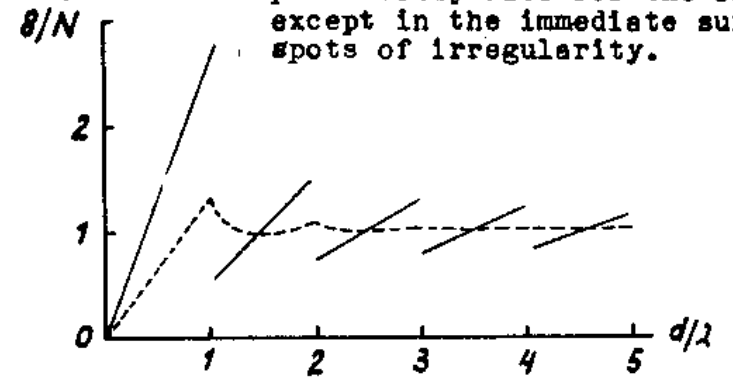

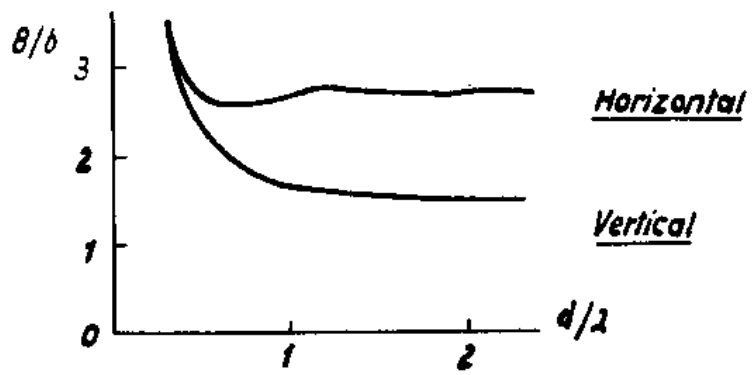

Fig. 5. Gain per unit length of the antenna with finite continuously excited horizontal and vertical arrays.

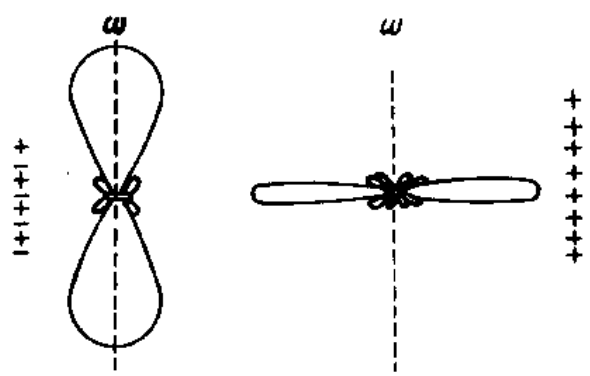

Fig. 6. Diagram of two equally long arrays of eight dipoles spaced d = 2/2 with direct phase and counter phase feeding.

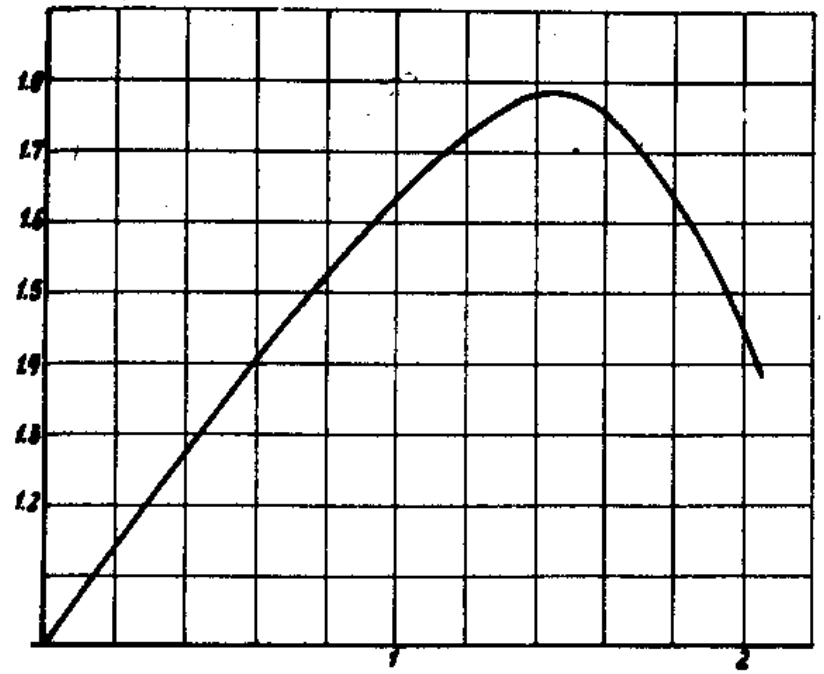

Fig. 7

The effective area at d - $\frac{\lambda}{2}$ is made equal to 1, L independent of d.

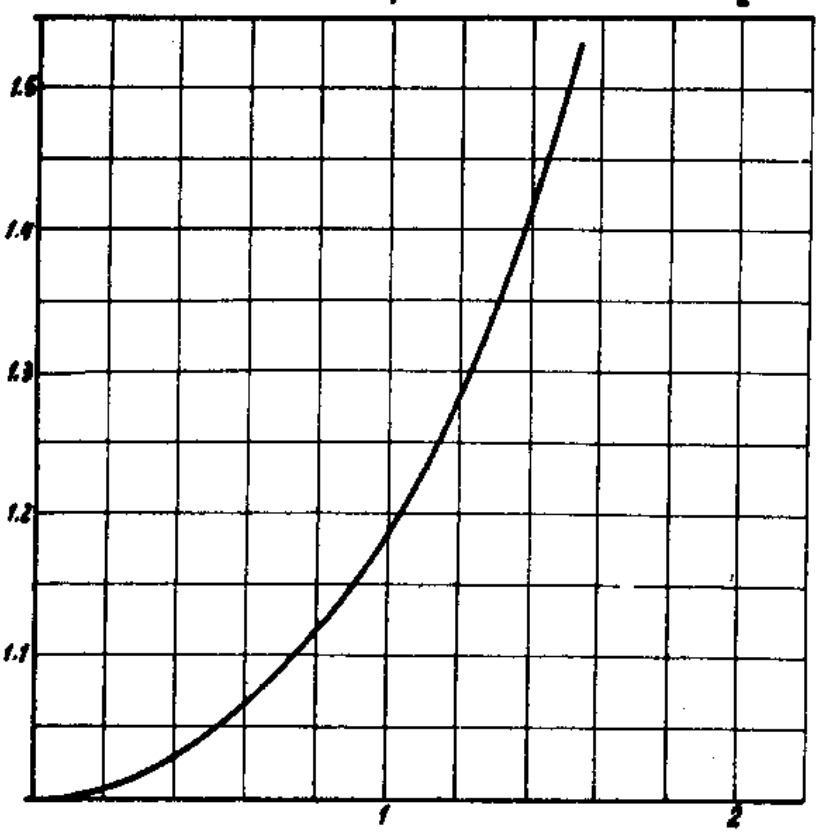

Fig. 7

Increase of the secondary lobes with respect to d = $\lambda/2$.

Increase of the effective area and secondary lobes in alternately fed dipole arrays as a function of the spacing d of two neighboring dipoles and of the length of the antenna L. The curves are valid also for di-electric antenna according to Mallaen and Zinke.

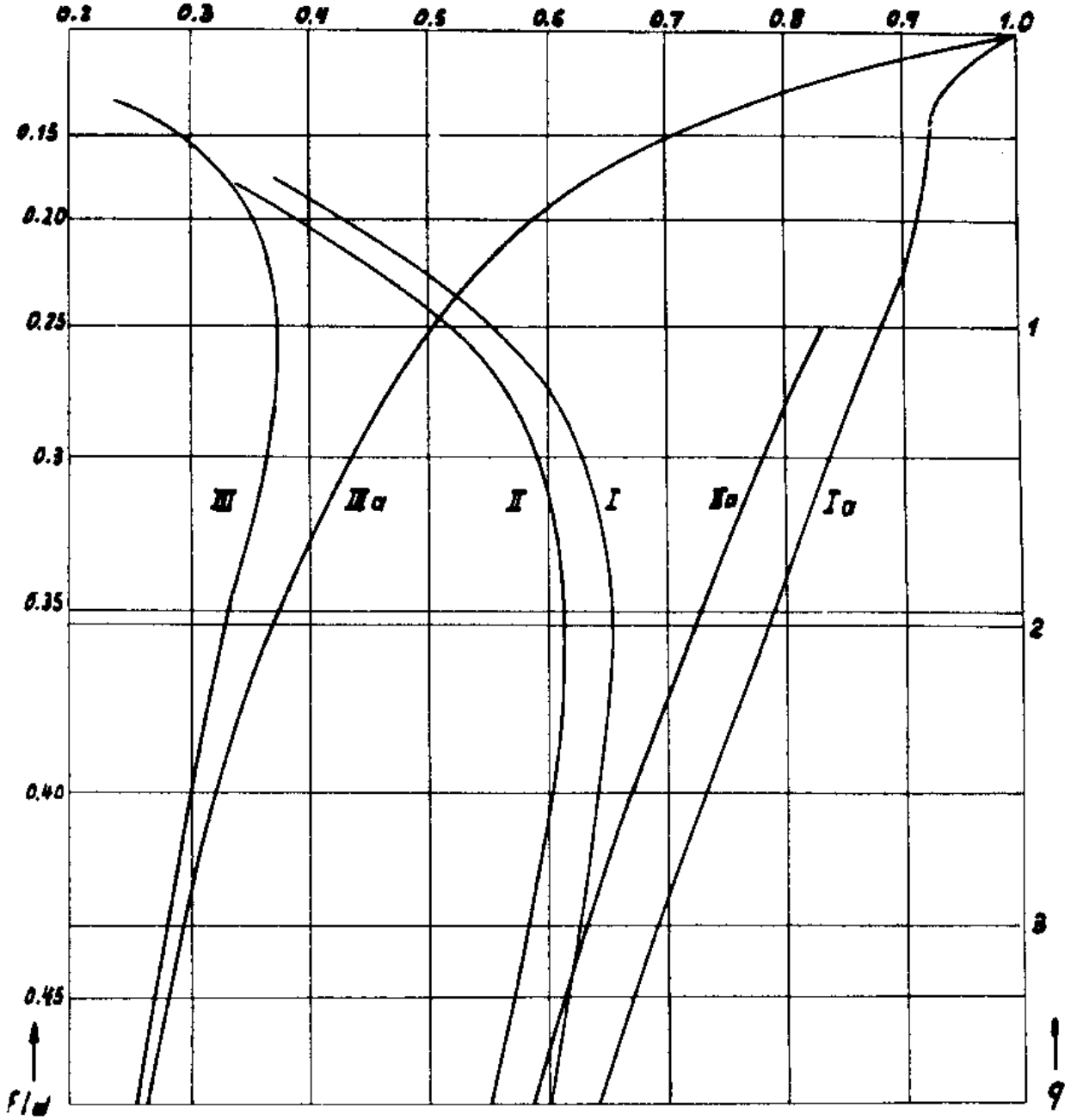

Fig. 8. Utilization of the Area of Parabolas

I. Dipole and reflector spaced $\frac{\lambda}{10}$

II. Dipole and reflector spaced $\frac{\lambda}{4}$

III. Dipole without reflector.

(a) The fraction of the total radiated output which is falling upon the mirror.

$$q = \frac{(4 \times \text{focal distance})^2}{(\text{mirror diameter})^2} = \frac{16\, f^2}{d^2}$$

q is a measure of the mirror shape;
$q >> 1$ means a plane mirror, at $q = 1$ the focal axis lies in the aperture plane.

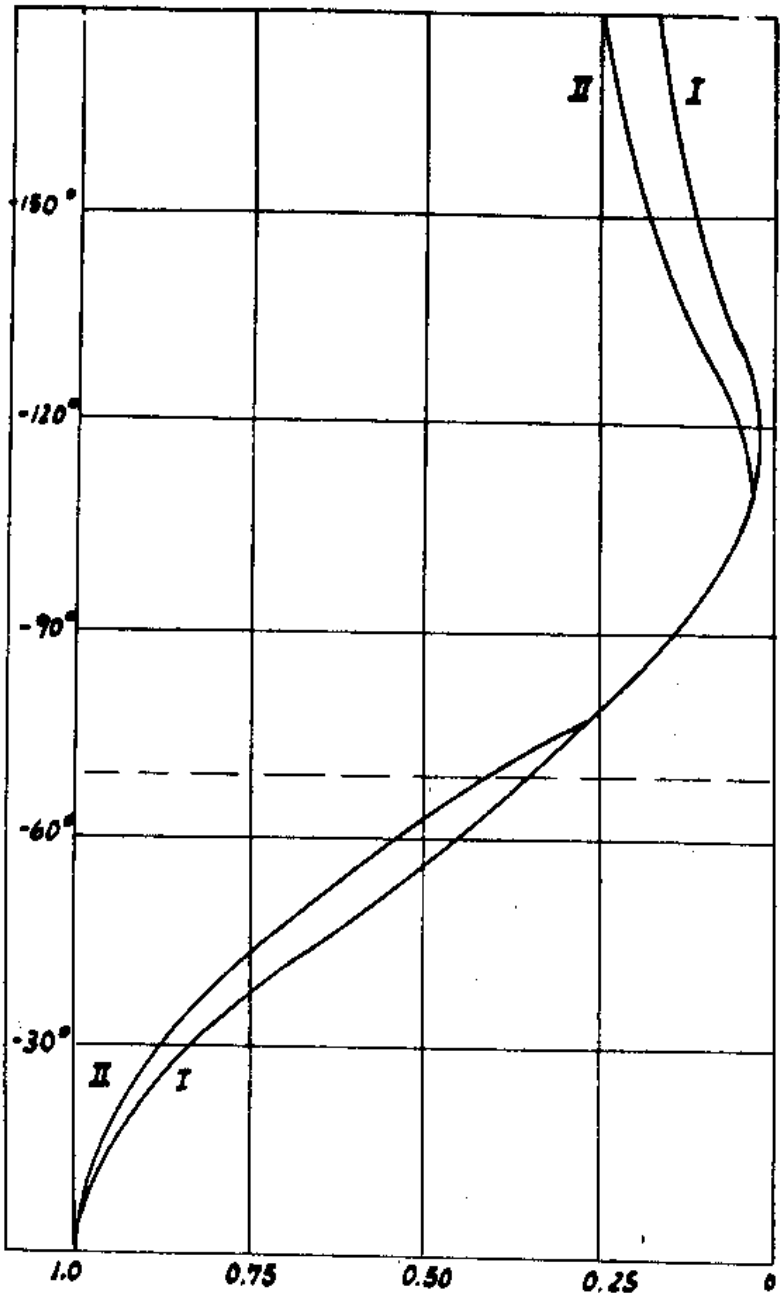

I Spacing dipole equal to $\lambda/10$

II Spacing dipole equal to $\lambda/4$

Most favorable location of the parabolic mirror in the diagram for prebunching.

FIG. 9. Output diagram of the combination of a dipole plus reflector which is used for the illumination of a parabolic mirror.

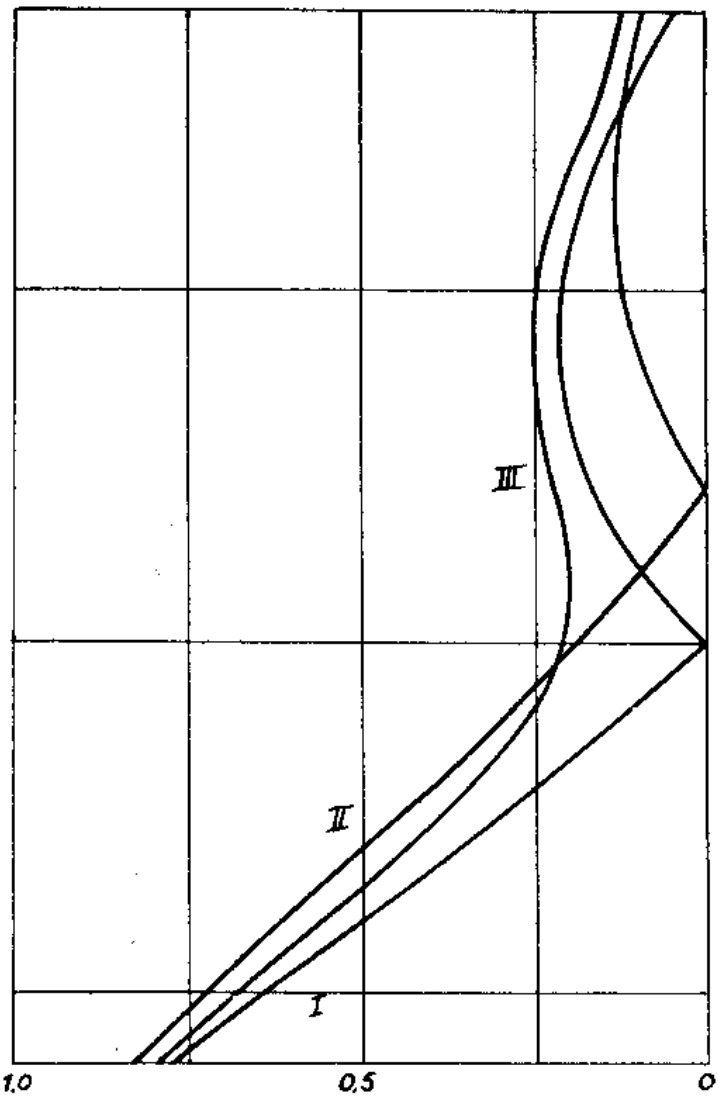

I. Dipole array
II. Parabolas
III. Slit radiators

Abscissae = Unit of angle
Ordinates = Field Intensity E

Figure 10. Field intensity diagram of dipole arrays and of continuously illuminated parabolic mirrors and slit radiators of optimum damping βl = 1.3 of the same length.

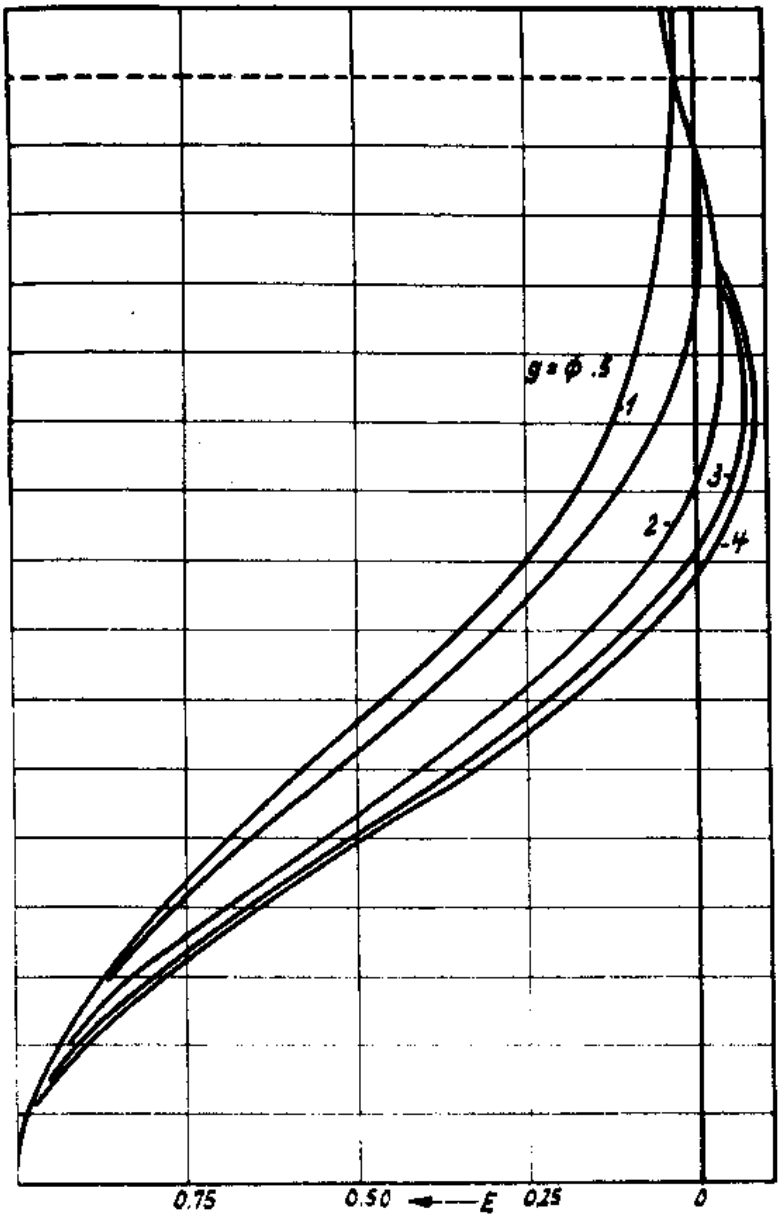

FIG. 11. Field intensity diagram of rotation parabolas with dipole in the focal point.

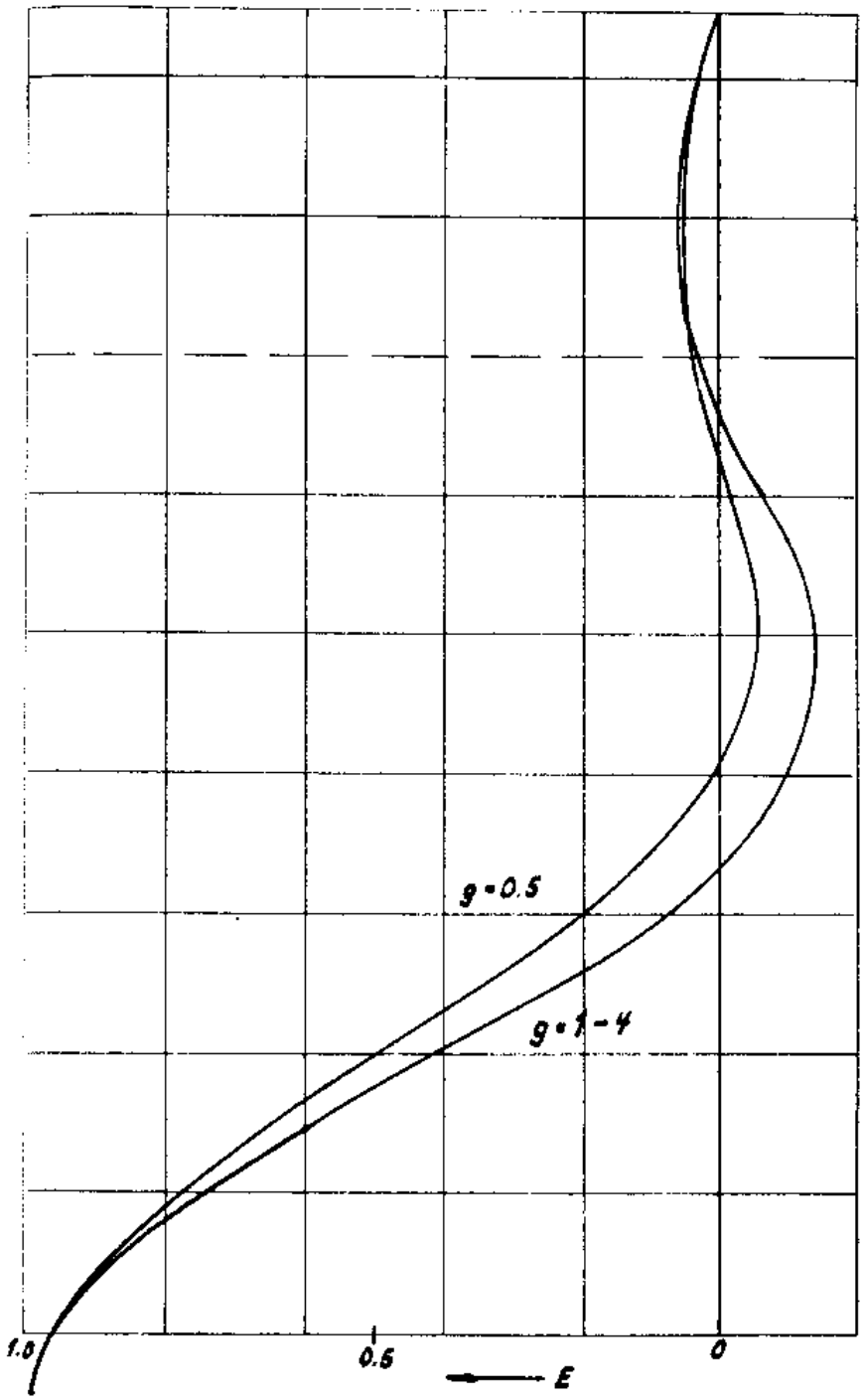

FIG. 12. Field intensity diagram for a rotation parabola with dipole in the focal axis.

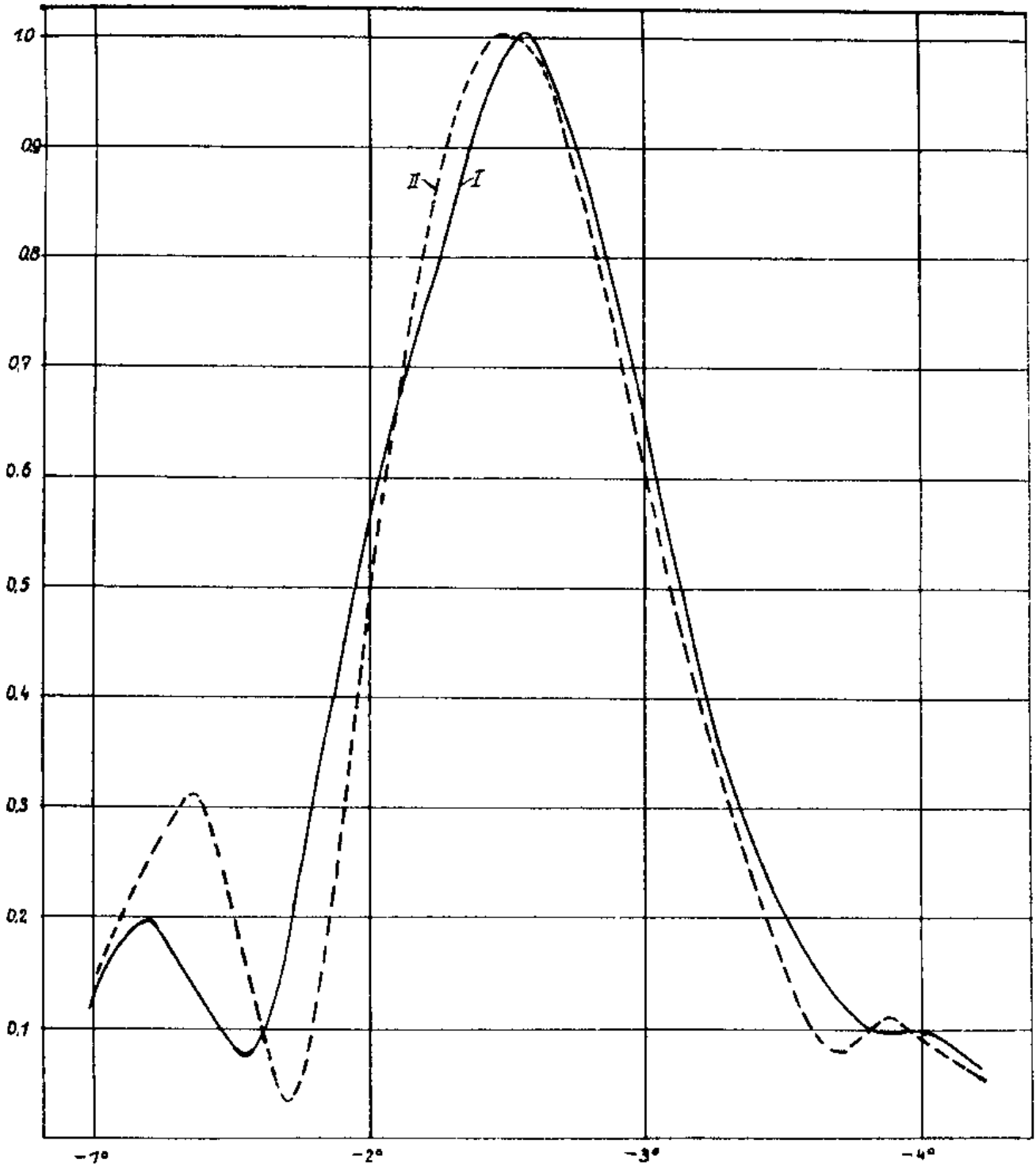

Fig. 13. Field intensity diagram of a rotation parabola with dipole and reflector. The dipole is radially defocused 3° in the direction of polarization in curve I and vertically in curve II. Mirror axis = 0°.

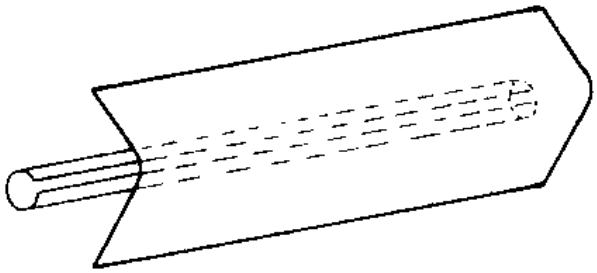

Fig. 14. Slit radiator in a cylindrical parabola.

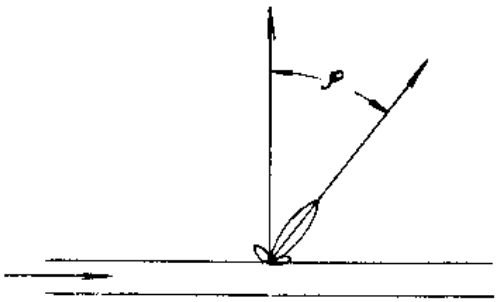

Fig. 15. Shifting of the slit radiator diagram towards the normal axis of the slit radiator.

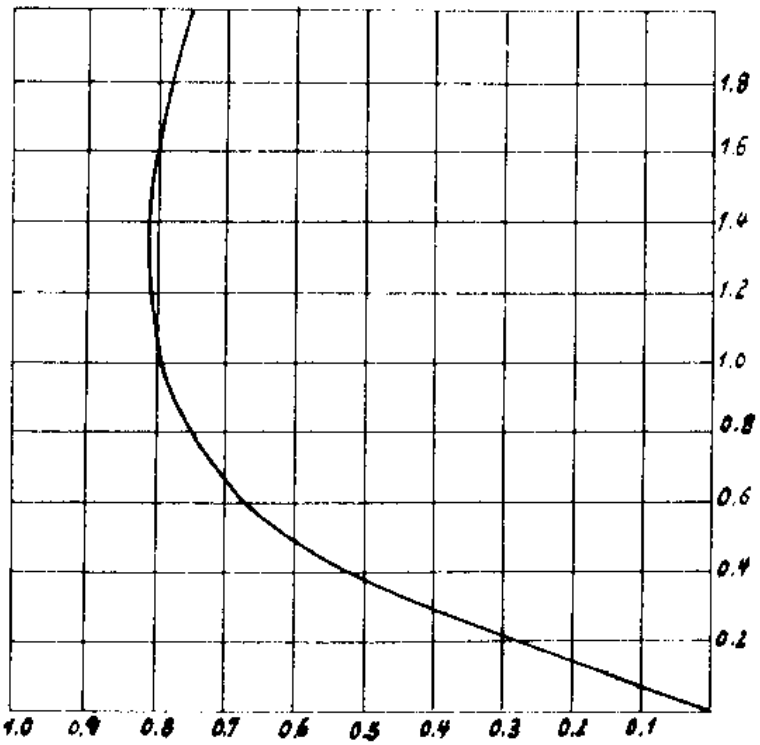

Fig. 16. Utilization of the area. Degree of effectiveness for slit radiators as a function of the totel damping L.

β = Damping constant
L = Length

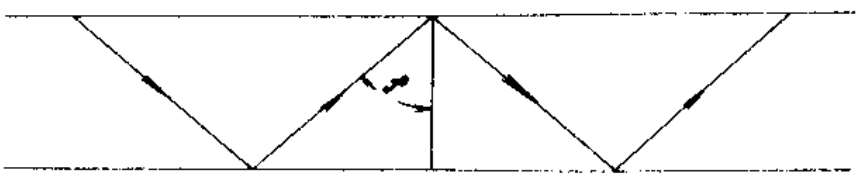

Fig. 17. The total reflection of a plane wave between the parallel boundaries of a di-electric.

May 02 D

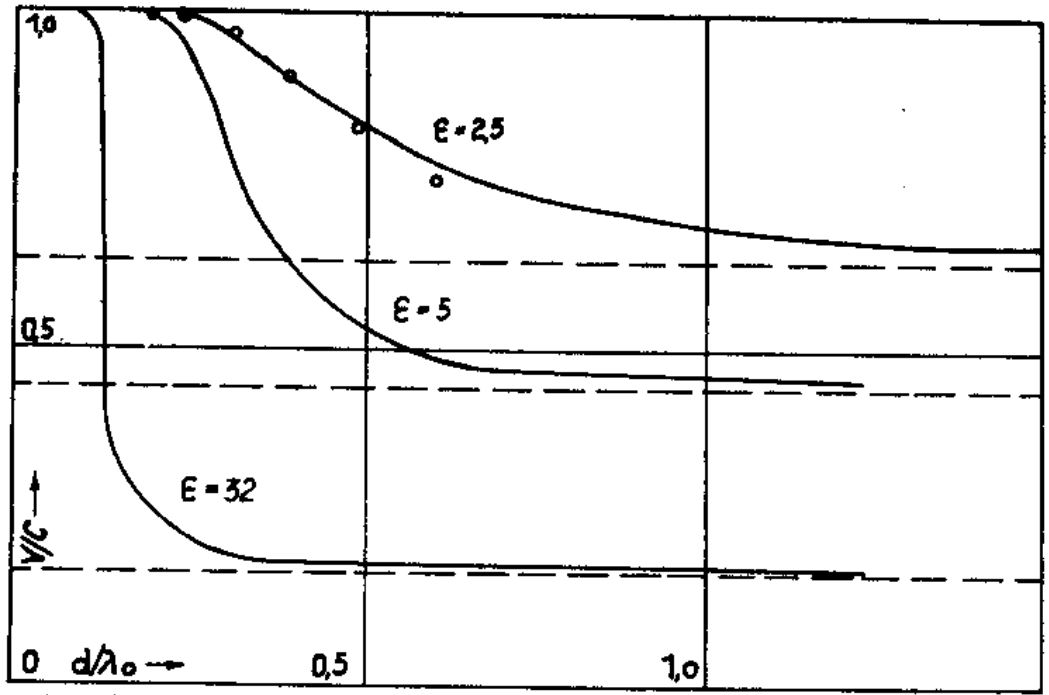

Fig. 18. Phase velocity of a simple type of wave which can be excited by a dipole on di-electric conductors according to measurements of Mallach and calculations of Wagener.

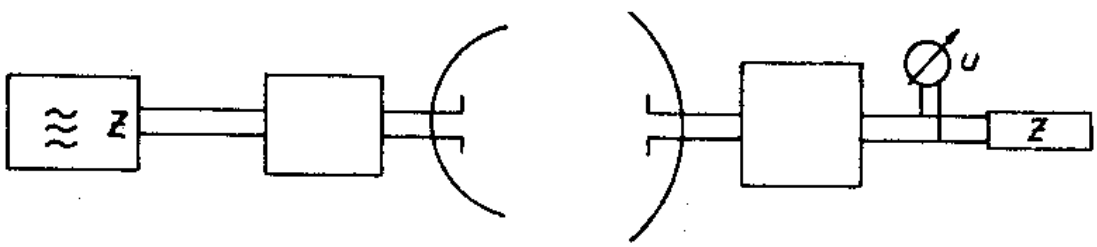

Fig. 19. Principle of absolute measurement of effective areas.

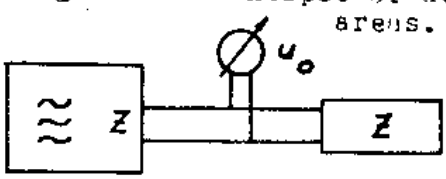

Fig. 20. Calibrated bridge for measuring impedance mismatching.

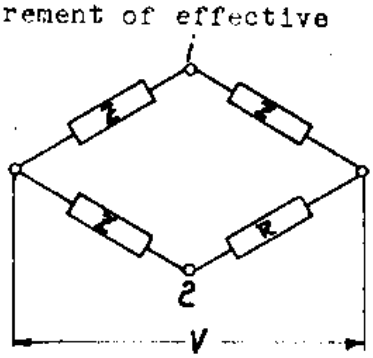

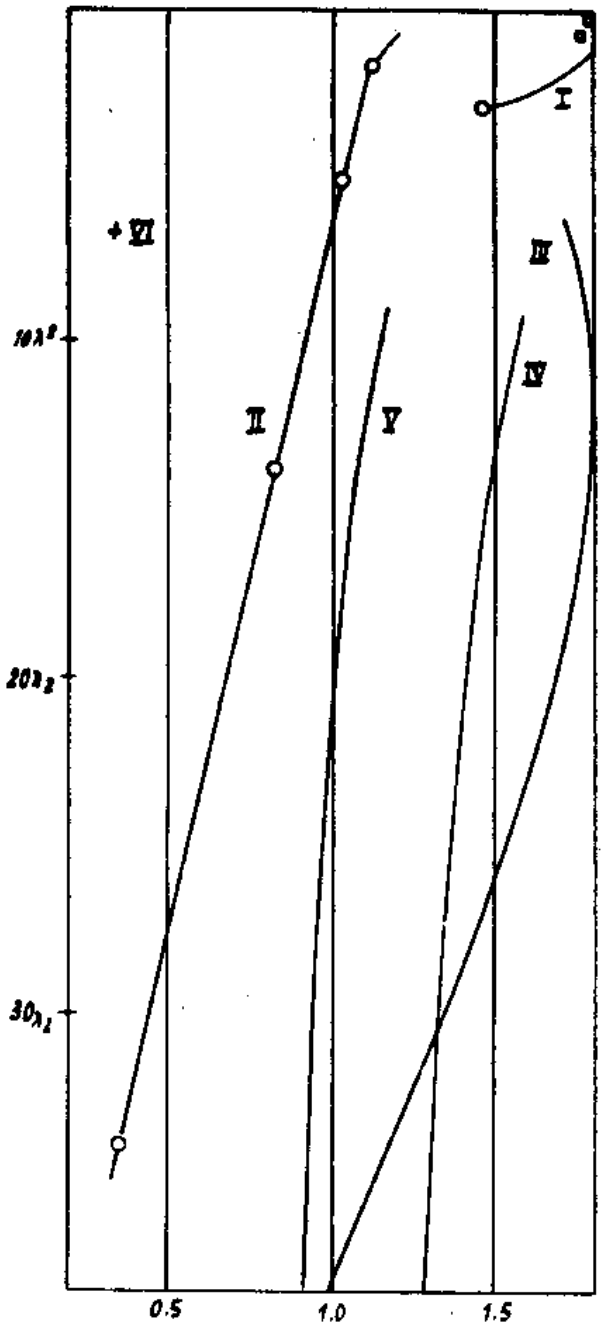

I. Round tubes according to Southworth and King.

II. Circular funnel according to Southworth and King, $2\alpha = 40^{\circ}$.

III. Square funnel according to Lamchen.

IV. Square funnels according to Stutzer, $2\alpha = 20^{\circ}$.

V. Square funnels according to Stutzer, $2\alpha = 40^{\circ}$.

VI. Circular funnels according to Schaeffer.

VII. Rectangular funnels according to Schaeffer.

Abscissae = Geometrical plane Fgeom of the funnel opening.

Ordinates = Utilization of the area.

Fig. 21. Utilization of the area of horn radiators according to measurements of various authors.

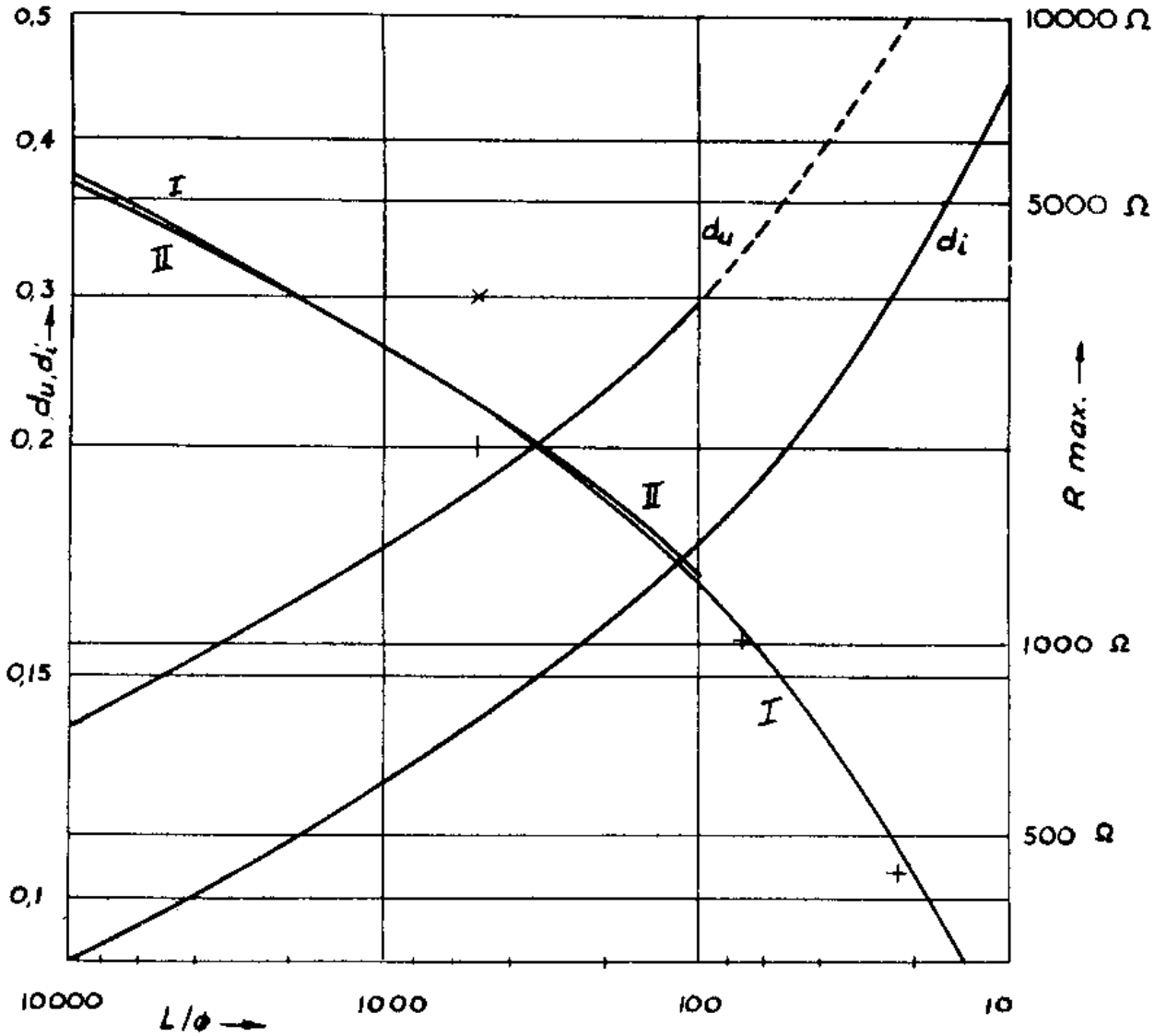

Effective resistance of dipoles in free space at the resonance voltage R_{max} damping at the voltage resonance d_u and at the current resonance d_i as a function of the slenderness ratio: $\frac{\text{Total length L}}{\text{Diameter } \phi}$

Fig. 22. R_{max} according to the line theory I and according to Hallens theory II and numerical calculation of Rothe.
Measured values of R_{max} +
Measured values of d_u x.

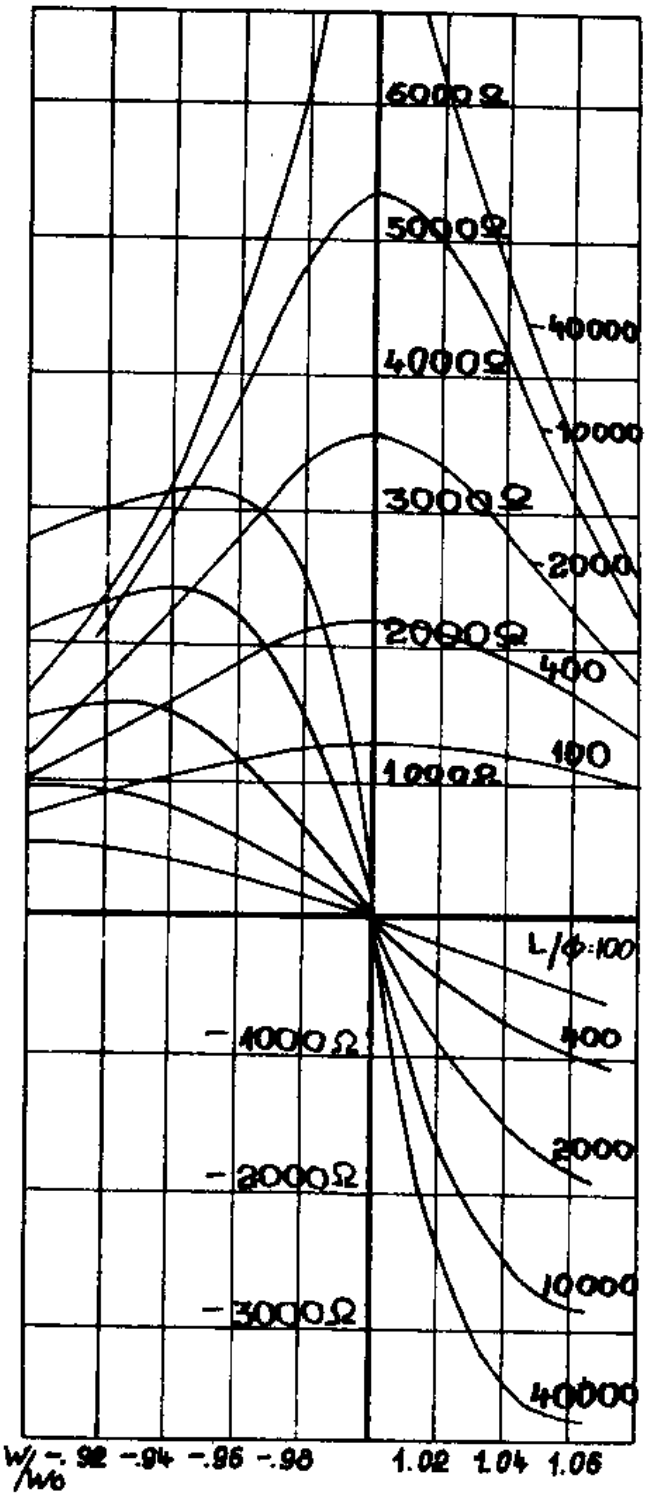

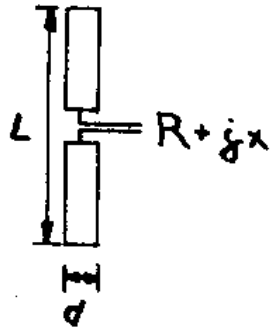

Fig. 22 a. Effective resistance and reactance of short wave dipoles in free space according to the Hallen theory as a function of the slenderness ratio $L/\varnothing$ and the detuning $\frac{\omega}{\omega_0}$.

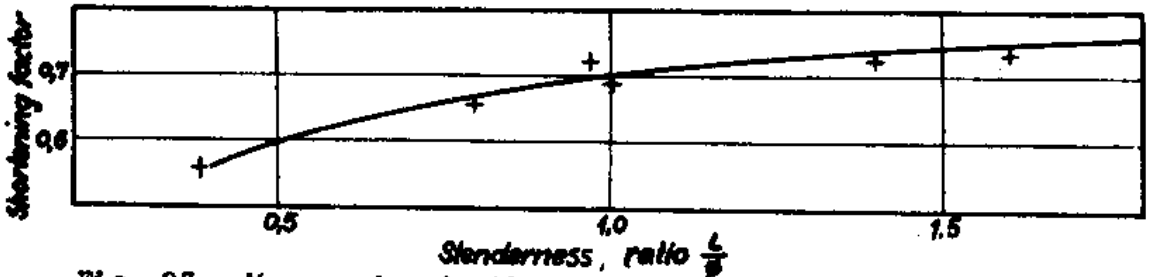

Fig. 23. Measured reduction factor of dipoles at voltage resonance

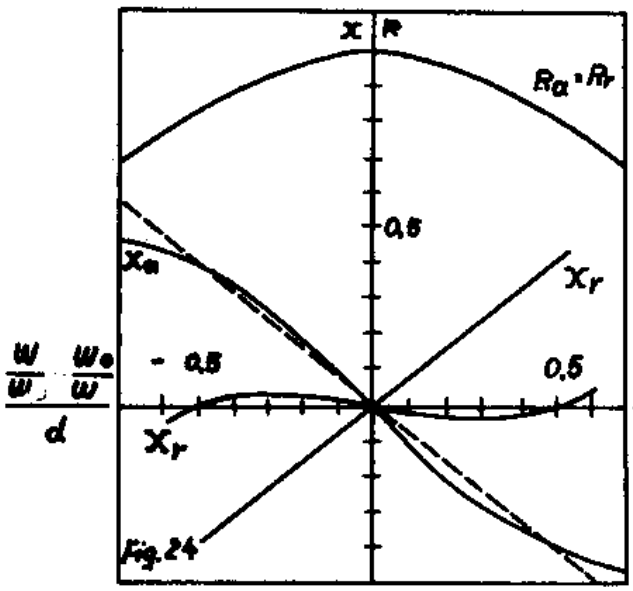

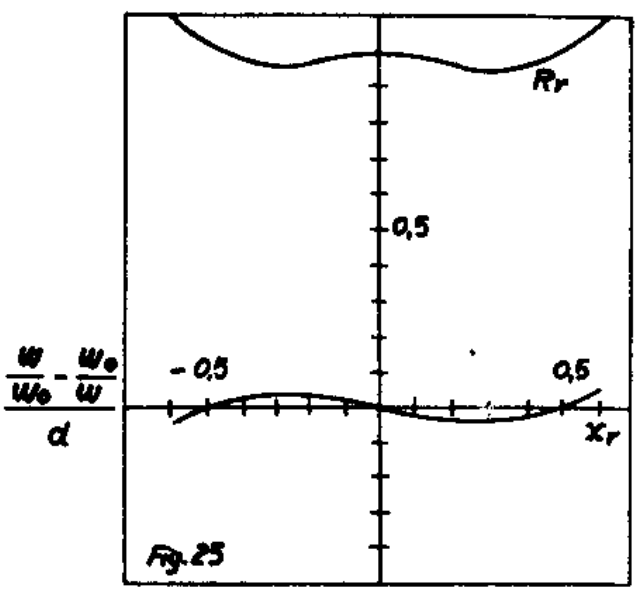

Fig. 24. Feeding of a dipole driven in voltage resonance to an L section. Effective resistance of a dipole R_a, Reactance of a dipole X, reactance of the added series circuit X_k and resulting effective resistance R_r, resulting reactance X_r. (d= Antenna damping)

Fig. 25. Resulting effective resistance and reactance by feeding the dipole with a π section. (d = Antenna damping)

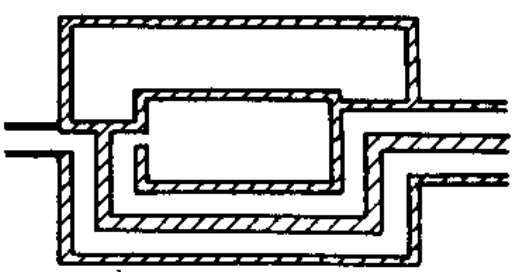

Fig. 27. Symmetrical Loop.

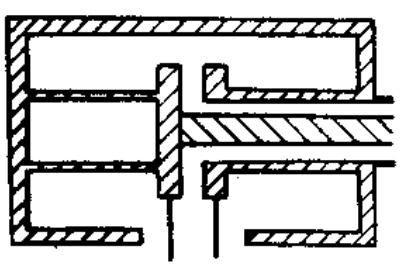

Fig. 26. Symmetrical chambe

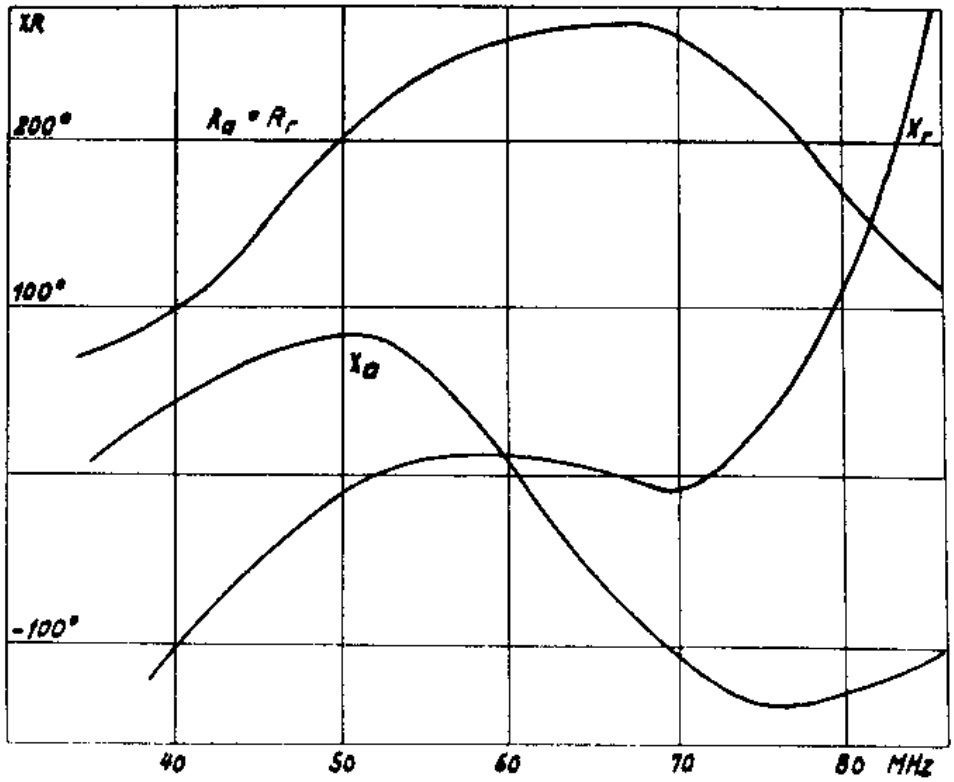

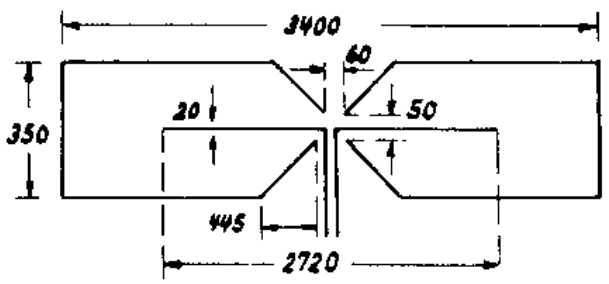

Fig. 26. Compensation of a dipole driven in voltage resonance by a built-in $\lambda/4$ circuit according to Buschbeck.